Environmental Science & Technology

pubs.acs.org/est

Article

Short-Term Exposure to Fine Particulate Matter and Ozone: Source Impacts and Attributable Mortalities

Song Liu, Xicheng Li, Jing Wei, Lei Shu, Jianbing Jin, Tzung-May Fu, Xin Yang, and Lei Zhu*

Cite This: *Environ. Sci. Technol.* 2024, 58, 11256−11267

Read Online

ACCESS | Metrics & More | Article Recommendations | Supporting Information

ABSTRACT: Short-term exposure to particles with aerodynamic diameters less than 2.5 μm ($PM_{2.5}$) and ozone (O_3) are important risk factors for human health. Despite the awareness of reducing attributable health burden, region-specific and source-specific strategies remain less explored due to the gap between precursor emissions and health effects. In this study, we isolate the health burden of individual sector sources of $PM_{2.5}$ and O_3 precursors, nitrogen oxides (NO_x) and volatile organic compounds (VOCs), across the globe. Specifically, we estimate mortalities attributable to short-term exposure using machine-learning-based daily exposure estimates and quantify sectoral impacts using chemical transport model simulations. Globally, short-term exposure to $PM_{2.5}$ and O_3 result in 713.5 (95% Confidence Interval: 598.8−843.3) thousand and 496.3 (371.3−646.1) thousand mortalities in 2019, respectively, of which 12.5% are contributed by fuel-related NO_x emissions from transportation, energy, and industry. Sectoral impacts from anthropogenic NO_x and VOC emissions on health burden vary significantly among seasons and regions, requiring a target shift from transportation in winter to industry in summer for East Asia, for instance. Emission control and health management are additionally complicated by unregulated natural influences during climatic events. Fire-sourced NO_x and VOC emissions, respectively, contribute to 8.5 (95% CI: 6.2−11.7) thousand and 4.8 (3.6−5.9) thousand $PM_{2.5}$ and O_3 mortalities, particularly for tropics with high vulnerability to climate change. Additionally, biogenic VOC emissions during heatwaves contribute to 1.8 (95% CI: 1.5−2.2) thousand O_3-introduced mortalities, posing challenges in urban planning for high-income regions, where biogenic contributions to health burden during heatwaves are 13% of anthropogenic contributions annually. Our study provides important implications for temporally dynamic and sector-targeted emission control and health management strategies, which are of urgency under the projection of continuously increasing energy consumption and changing climate.

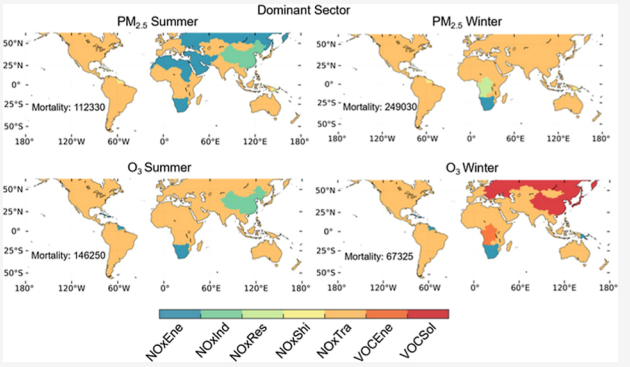

KEYWORDS: *air pollution, health burden, precursor impacts, machine learning, chemical simulation*

1. INTRODUCTION

Air pollution is the fourth highest risk factor for global mortality, with 4.1 million and 0.4 million caused by long-term exposure to ambient particulate matter (aerodynamic diameter less than 2.5 μm, $PM_{2.5}$) and ozone (O_3), respectively, in 2019.[1] Major sources of $PM_{2.5}$ and O_3 include formation through photochemical reactions involving precursors nitrogen oxides (NO_x) and volatile organic compounds (VOCs), both of anthropogenic and natural origins.[2] To develop promising mitigation measures, source attribution of long-term concentrations of O_3 and $PM_{2.5}$ has been reported extensively.[3,4] However, acute health effects and the source attribution of short-term exposure to $PM_{2.5}$ and O_3 remain less studied, particularly on a global scale, leaving a gap between precursor control and health management. This study provides a globally comprehensive source categorization of the $PM_{2.5}$ and O_3 health burden attributable to their short-term exposure.

Despite efforts on emission control in recent years, highly polluted days are still frequently reported in urbanized and industrialized regions, with $PM_{2.5}$ or O_3 concentrations exceeding the World Health Organization (WHO) recommended daily air quality guidelines (AQG) levels.[5−8] Premature mortalities attributable to short-term $PM_{2.5}$ or O_3 exposure are regionally estimated at up to 108.9 thousand per year.[9,10] Aside from anthropogenic sources, climatic events such as wildfires and heatwaves are episodically associated with spiked $PM_{2.5}$ or O_3 concentrations[11−13] along with health burden.[14−17]

Received: January 10, 2024
Revised: June 3, 2024
Accepted: June 4, 2024
Published: June 17, 2024

Comprehensive tracking of the pollution health burden requires high-quality pollution exposure data. Researchers commonly use ground-based measurements, satellite retrievals, or chemical transport model simulations to estimate $PM_{2.5}$ and O_3 health burden.[4,10,18,19] The recent integration of these multiple data sources using machine learning models appears attractive,[9,20,21] with high accuracy, fine resolution, and full coverage.

On top of pollution exposure data, assessments of sources and impacts are important in light of policy strategies. Source attribution of long-term $PM_{2.5}$ and O_3 pollution is widely implemented using the tagging approach[3,22,23] and the zeroing-out approach.[4,24] While the tagging method involves labeling or tagging modeled $PM_{2.5}$ or O_3 with the identity of the emitted precursors, which produces information about the contribution of different precursors to $PM_{2.5}$ or O_3 in a simulation, the zeroing-out method perturbs emissions from a given source sector in sensitivity simulations along with a baseline simulation, which gives information about the response of $PM_{2.5}$ or O_3 to changes in precursor emissions.[3] Both methods provide source−receptor relationships between precursor emissions and pollutant concentrations, with the former focusing on contributions (source apportionments) and the latter on impacts (source sensitivities).[25]

In this study, we derive daily full-coverage machine learning estimates for ambient $PM_{2.5}$ and O_3 concentrations and investigate the mortalities attributable to their short-term exposure in 2019. Moreover, we apply the zeroing-out method, on the basis of chemical transport model sensitivity simulations, to quantify influences from individual NO_x and VOC emission sectors for polluted days, including climatic events such as fires and heatwaves. Such insights from a global perspective are particularly important to customize strategic policies with the greatest public health benefits.

2. DATA AND METHODS

2.1. Global Daily $PM_{2.5}$ and O_3 Exposure Estimates. We assess short-term $PM_{2.5}$ and O_3 exposure as daily average $PM_{2.5}$ concentrations and daily maximum 8 h average (MDA8) O_3 concentrations, and we derive pollution concentrations using satellite gap-filled data and machine learning at a 10×10 km^2 resolution.[20,21] Input data include ground-based in situ observations, satellite remote sensing products, reanalysis products of meteorological parameters and trace gas concentrations, emission inventories, population density, economic level, land cover, and terrain changes. See Text S1 for details of the data sources.

We adopt a tree-based ensemble-learning extremely randomized trees (extra-trees)[26] for modeling air pollutants, with unique advantages including stronger randomness and an anti-interference ability.[5] Specifically, a four-dimensional space-time extra-trees (4D-STET) model is developed by introducing Euclidean spherical space and triangular spiral time to better describe both the autocorrelations and differences of individual points in spatial locations (e.g., different global hemispheres) and temporal series (e.g., seasonal cycles). Within the 4D-STET framework, assimilation data are first used to fill satellite gaps over cloudy scenes and snow/ice cover, and afterward, surface concentrations are estimated based on input data.

The daily gap-filled data achieve similar validation results to retrievals without gap-filling (with a 1% reduction in correlation coefficients relative to ground-based measurements) and increase the daily spatial coverage by 36%, accompanied by a nearly 3-fold expansion in the training sample size.[21] The performance of daily exposure estimates is evaluated with sample-based 10-fold cross-validation (Figure S1). The machine learning data, in line with ground-based observations with high cross-validated coefficients of determination (>0.89), low root-mean-square error (<9.1 $\mu g\ m^{-3}$), and low mean absolute error (<5.8 $\mu g\ m^{-3}$), show great prediction ability in daily and global manners and act as a firm basis for our health burden estimation.

2.2. Health Burden Due to Short-Term Exposure to $PM_{2.5}$ and O_3. We estimate premature mortalities attributed to short-term exposure $\Delta Mort$ with the human health impact function[27,28] as

$$\Delta Mort = y_0 \sum_i \sum_j Pop_i[1 - RR(\Omega_{i,j})^{-1}] \quad (1)$$

For each global burden of disease (GBD) region, y_0 is the daily baseline mortality rate in 2019 (https://vizhub.healthdata.org/gbd-results). $RR(\Omega_{i,j})$ is a log−linear concentration−response function[29] relating the change in surface air pollutant concentration Ω to the change in relative risk RR for i grid on j day. We use RR for all-cause mortality as 1.0065 (95% Confidence Interval [CI]: 1.0044−1.0086) for $PM_{2.5}$ and 1.0043 (1.0034−1.0052) for O_3 with an increase in pollutant concentration per 10 $\mu g\ m^{-3}$ following a short-term study.[30] Theoretical minimum-risk concentrations without adverse health impacts are selected from the GBD study.[1] The population Pop is from Gridded Population of the World (GPW) v4 (http://sedac.ciesin.columbia.edu/data/collection/gpw-v4). The daily mortality estimates are added up into annual sums for result discussions. Uncertainties of health burden estimates are calculated considering ranges in baseline mortality rates and theoretical minimum-risk concentrations.[1,30]

2.3. Simulated Fractional Sector Impacts. We derive the fractional sector impacts from a series of perturbation simulations using the chemical transport model GEOS-Chem version 12.9.3 (http://www.geos-chem.org) driven by Modern-Era Retrospective Analysis for Research and Applications, Version 2 (MERRA-2) meteorological fields.[31] With a spin-up time of 1 year, the global simulations are configured at a resolution of $2° \times 2.5°$ with 47 vertical layers. Anthropogenic emissions for 2019 are from the Community Emissions Data System (CEDS) inventory at a resolution of $0.1° \times 0.1°$.[32] Soil NO_x emissions from the natural nitrogen pool and fertilizer input are calculated using the Berkeley-Dalhousie Soil NO_x Parameterization (BDSNP) in GEOS-Chem.[33] Biogenic emissions are calculated online using the Model of Emissions of Gases and Aerosols from Nature (MEGAN) version 2.1.[34] Biomass burning emissions are from the fourth-generation Global Fire Emissions Database (GFED4).[35] GEOS-Chem simulations are interpolated to grids of exposure data using the bilinear interpolation method.

GEOS-Chem includes a coupled treatment of O_3−NO_x-VOC-aerosol-halogen chemistry[36−39] and uses a bulk aerosol scheme with fixed log−normal modes.[40] $PM_{2.5}$ is simulated in GEOS-Chem as the sum of sulfate-nitrate-ammonium (thermodynamic equilibrium computed with ISORROPIA II),[41,42] organic aerosol,[43] black carbon,[44] dust,[45] and sea salt[46] components. We use a volatility basis-set approach for nonisoprene secondary organic aerosols and an explicit aqueous uptake mechanism to model isoprene secondary organic aerosols.[43]

The GEOS-Chem model reproduces main patterns for trace gases with biases generally lower than 50%, evaluated against

https://doi.org/10.1021/acs.est.4c00339
Environ. Sci. Technol. 2024, 58, 11256−11267

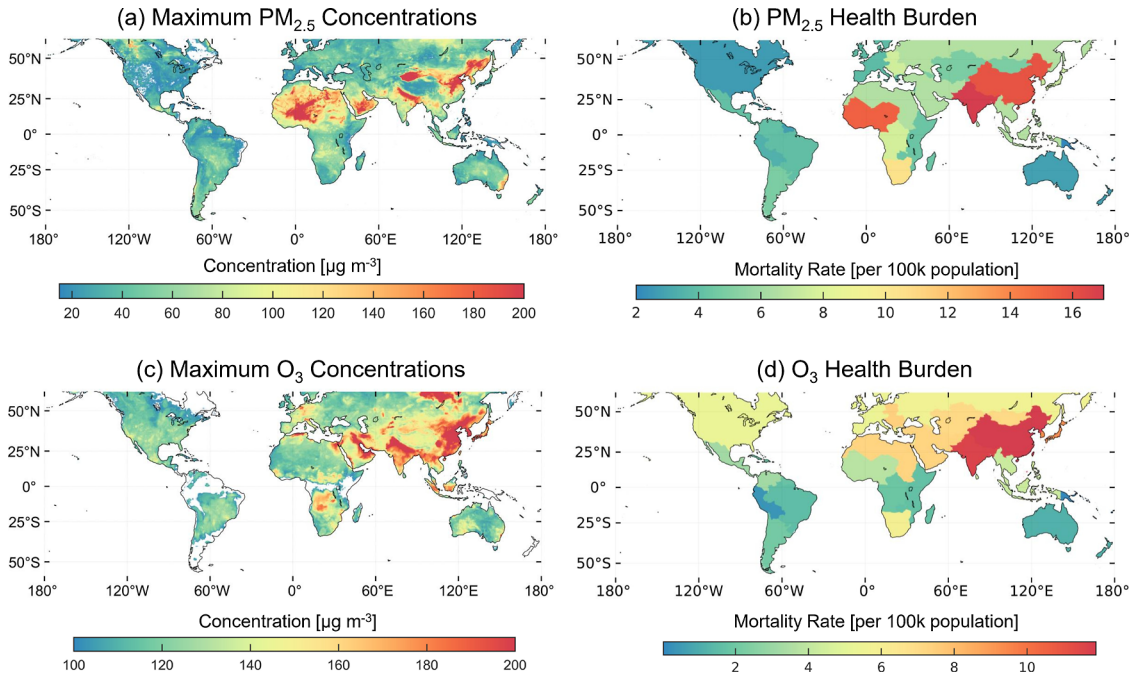

Figure 1. Maximum values of daily $PM_{2.5}$ and daily maximum 8 h average (MDA8) O_3 concentrations and region-level mortality rates attributable to short-term pollution exposure in 2019. Concentrations below WHO AQG levels are not shown in (a,c). See Figure S4 for grid-based estimates of (b,d).

extensive space-, aircraft-, and ground-based observations.[47−49] We show in Figures S2 and S3 that our GEOS-Chem simulations agree with in situ observations, with correlation coefficients larger than 0.75 and biases lower than 38.6% (annual values for $PM_{2.5}$ and summer values for O_3). The biases are mainly related to the uncertainties in anthropogenic and natural emission estimates as well as parametrization resolutions for meteorology or chemical processes.[50]

We apply the zeroing-out technique, where fractional $PM_{2.5}$ and O_3 mass impacts are calculated as relative differences between the base and sensitivity simulations that systematically remove individual source sectors. From that, population-weighted fractional source contributions F_{source} for each GBD region are calculated by dividing those source impacts *Frac* by the total population-weighted mean concentrations as

$$F_{source} = \sum_j \frac{\sum_i Frac_{i,j} \times C_{i,j} \times Pop_i}{\sum_i Pop_i} \Big/ \frac{\sum_i C_{i,j} \times Pop_i}{\sum_i Pop_i} \quad (2)$$

where $C_{i,j}$ is the $PM_{2.5}$ or O_3 concentration for *i* grid on *j* day. F_{source} are then applied to the health burden in eq 1 to calculate source impacts from each sector. Anthropogenic source sectors for NO_x and VOCs cover transportation, energy, ships, residential, industrial, solvents, agriculture, and waste. Natural source sectors include soil NO_x, lightning NO_x, fire NO_x, biogenic VOCs, and fire VOCs.

Note that the zeroing-out method quantifies the source sensitivities to air pollutants, which include the interaction of each specific source with all other sources rather than the pure impact from the specific source alone.[24,51] CEDS sectors with higher levels of uncertainty include waste burning, residential emissions, and agricultural processes due to the difficulty in accurately tracking energy consumption statistics and uncertainties in the variability in source-specific emission factors.[32,52] However, the above sectors play relatively less important roles in our analysis (see Section 3.2). Additionally, due to the use of relative differences in describing sectoral emission impacts, the method is less sensitive to the absolute values of GEOS-Chem simulations, as analyzed in our previous works.[53,54]

3. RESULTS AND DISCUSSION

3.1. Short-Term Exposure and Attributable Health Burden. In 2019, 97.5 and 87.1% of the global population experience, respectively, $PM_{2.5}$ and O_3 pollution, exceeding daily AQG levels (15 $\mu g\ m^{-3}$ for $PM_{2.5}$ and 100 $\mu g\ m^{-3}$ for O_3)[55] in Figure 1. The values are 25.4 and 14.9% for Interim 1 targets (75 $\mu g\ m^{-3}$ for $PM_{2.5}$ and 160 $\mu g\ m^{-3}$ for O_3), an initial stage toward the attainment of the final AQG target. The daily $PM_{2.5}$ concentration can reach 631.2 $\mu g\ m^{-3}$, and the O_3 concentration peaks at 357.3 $\mu g\ m^{-3}$. Spatially, top $PM_{2.5}$-introduced mortality rates are noticed in South Asia (18.2 [95% CI: 15.9−20.6] per 100 thousand population), East Asia (15.8 [13.2−18.8]), and Western Sub-Saharan Africa (15.3 [12.8−18.4]). During the same time, the top O_3-attributable mortality rates are located in East Asia (11.9 [95% CI: 9.1−15.2] per 100 thousand population), South Asia (11.6 [9.1−14.4]), and High Income Asia Pacific (9.3 [7.3−11.4]).

Globally, short-term $PM_{2.5}$ and O_3 exposure cause a total of 713.5 (95% CI: 598.8−843.3) and 496.3 (371.3−646.1) thousand mortalities (Figure 2). Driven by prolonged pollution episodes and high concentrations, both $PM_{2.5}$ and O_3 pose significant challenges for health management in South Asia and East Asia, together accounting for 66.0% of global mortalities on average. Compared to previous regional studies focusing on China,[9,10] our mortality estimates in East Asia show higher values by more than 1.8 times (Table S4), due to the use of stricter theoretical minimum-risk concentrations and higher relative risk.

Meanwhile, the O_3 health burden can be greater than that of $PM_{2.5}$ by up to a factor of 2 for high-income regions, including Western Europe, High Income North America, and High Income Asia Pacific. High $PM_{2.5}$- and/or O_3-mortalities in such

https://doi.org/10.1021/acs.est.4c00339
Environ. Sci. Technol. 2024, 58, 11256−11267

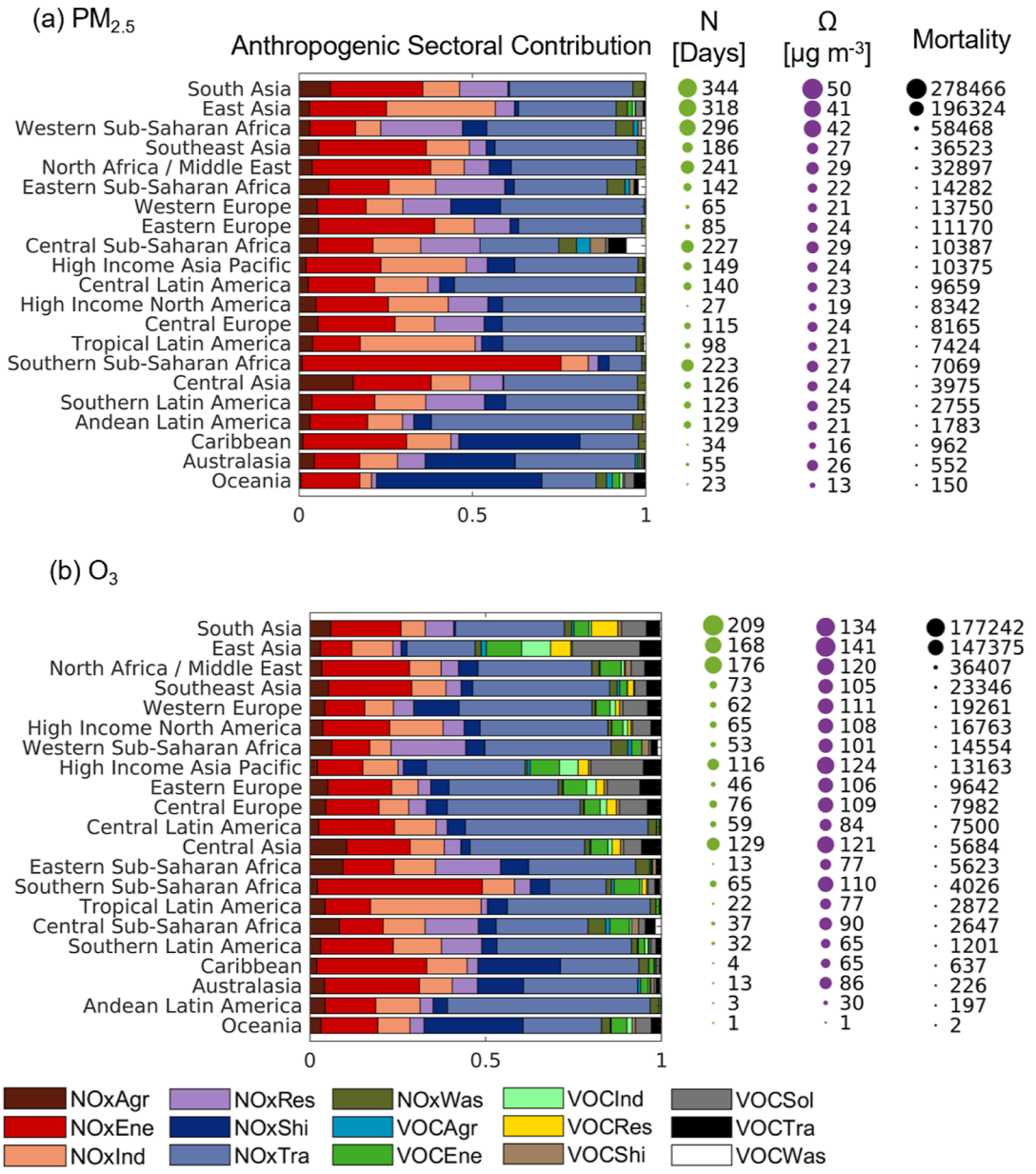

Figure 2. Normalized sectoral impacts on $PM_{2.5}$- and O_3-attributed mortalities from anthropogenic NO_x and VOC emissions. Sectors are shown for agricultural (Agr), energy (Ene), industrial processes (Ind), residential (Res), ships (Shi), transportation (Tra), and waste (Was). Negative influences are excluded from the analysis. Population-weighted mean polluted days exceeding WHO AQG levels (N), population-weighted mean $PM_{2.5}$ and MDA8 O_3 concentrations for polluted days (Ω), and attributable mortalities are sorted by decreasing values of mortalities. Dot sizes show relative amounts. See Table S1−S3 for the numbers of sectoral contributions to mortalities.

regions, despite the relatively shorter durations of polluted days and lower levels of pollution exposure, reflect differences in population density, baseline mortality rate, urban-rural structure,[56] and local emission source.

3.2. Anthropogenic Sources. Large $PM_{2.5}$ health burden is typically accompanied by high anthropogenic NO_x contributions (up to 28.8%) in populated regions across the northern hemisphere (Figure 3). For these areas, anthropogenic emissions also contribute largely to O_3-attributable mortalities (up to 31.6% for NO_x and 13.7% for VOC). Globally, anthropogenic NO_x emissions result in 192.4 (95% CI: 155.5−237.2) thousand mortalities (103.3 [87.2−121.1] thousand for $PM_{2.5}$ and 89.1 [68.3−116.1] thousand for O_3), and anthropogenic VOC contributions additionally lead to 39.1 (29.4−50.0) thousand O_3-related mortalities (Tables S1−S3). Meanwhile, natural NO_x and VOC emissions can offset the emission control efforts and health benefits due to their large influences (seasonally by up to 56.3%; Figures 3 and S5) and possible synergetic or competitive relationships with anthropogenic sources.[57] Aside from the above secondary emissions from atmospheric chemical reactions between NO_x and VOCs, the remaining sources of $PM_{2.5}$ (regionally by more than 64.3%; Figure 3) largely correspond to direct emissions, such as forest fires and agricultural waste burning, windblown mineral dust from arid regions, and inefficient fuel combustion.[4]

Among anthropogenic sectors in Figure 2 and Tables S1−S3, transportation from NO_x emissions plays the most important role in global health burden attributable to short-term exposure (35.4 [95% CI: 29.9−41.5] thousand for $PM_{2.5}$ and 37.0 [28.2−48.2] thousand for O_3), followed by energy (26.0 [22.1−30.4]

https://doi.org/10.1021/acs.est.4c00339
Environ. Sci. Technol. 2024, 58, 11256−11267

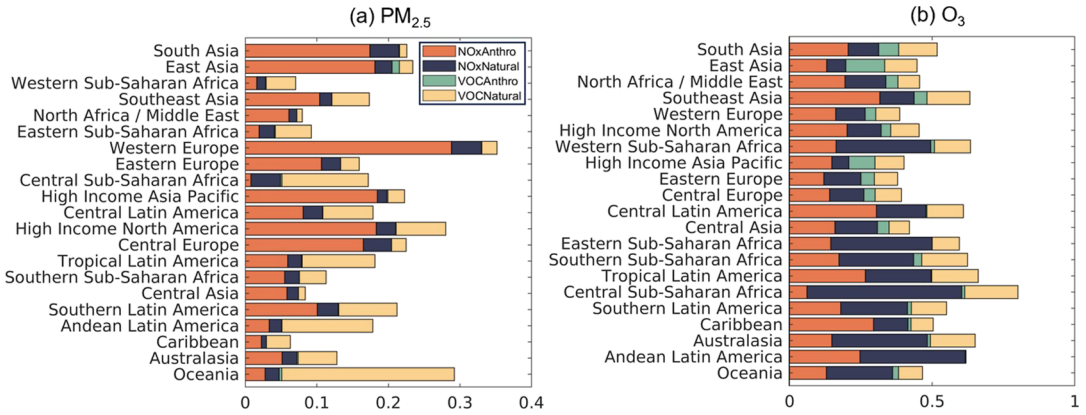

Figure 3. Fractional contributions from anthropogenic and natural NO_x and VOC emissions to $PM_{2.5}$- and O_3-attributed mortalities. Regions are sorted by decreasing values of mortalities following Figure 2.

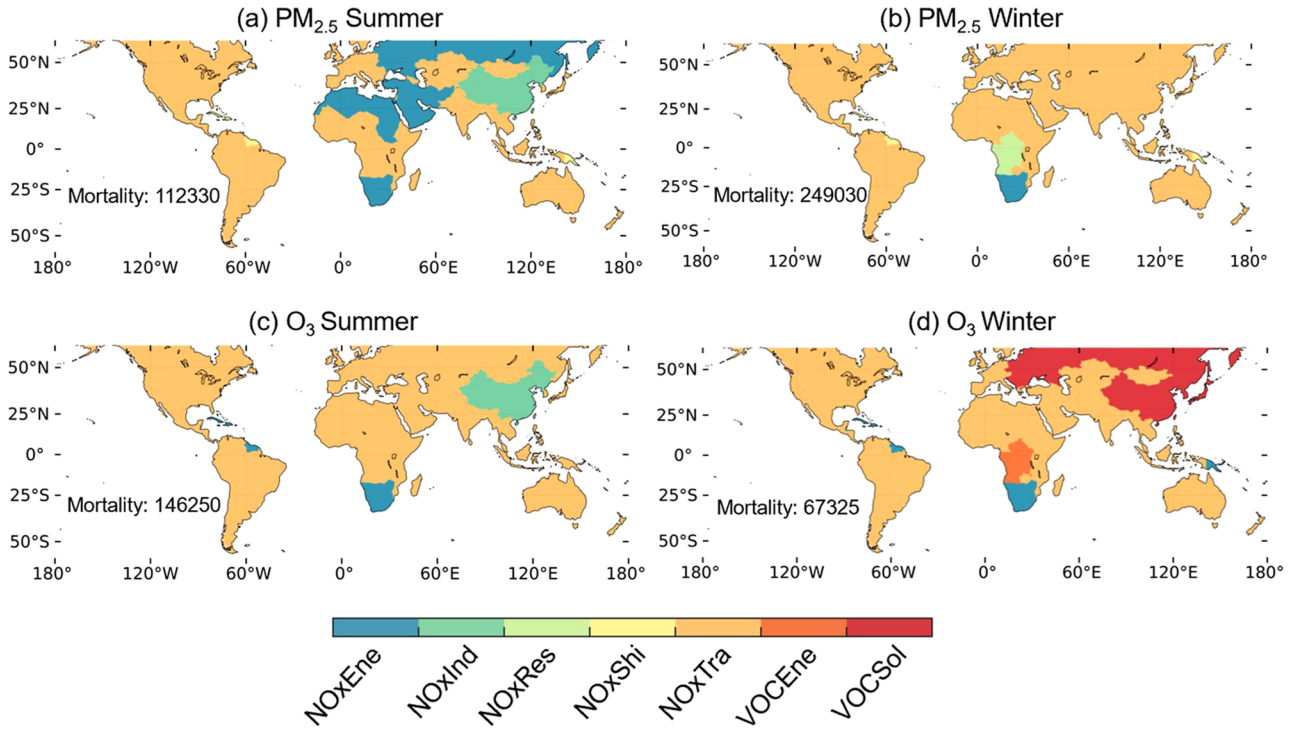

Figure 4. Dominant anthropogenic sector with the largest relative contribution to mortalities attributable to short-term $PM_{2.5}$ and O_3 exposure for summer and winter in 2019. Sectors for anthropogenic NO_x and VOC emissions are analyzed in Figure 2. Total $PM_{2.5}$- and O_3-related mortalities are given inset.

thousand and 21.2 [16.4−27.5] thousand) and industry (19.6 [16.4−23.1] thousand and 12.1 [9.7−15.7] thousand). These three NO_x sources, which are typically associated with fuel combustion, together account for 12.5% of the total $PM_{2.5}$ and O_3 health burden. Besides, anthropogenic VOC emissions from the solvent, energy, and residential sectors result in 5.4% of the O_3-related mortalities worldwide, with each contributing to 12.9 (95% CI: 9.7−16.5) thousand, 7.7 (5.7−9.8) thousand, and 6.4 (4.7−8.0) thousand mortalities. Smaller global sectors, such as agriculture, shipping, and waste, are potentially important for regional control strategies. We note that the impacts of agricultural practices can be underestimated in this work. Due to the combined influences of both agricultural management and meteorological variables, the distinctions between natural and anthropogenic contributions are usually difficult for soil emissions. Here, we follow the common practice of anthropogenic sectors from the CEDS inventory, in which agricultural NO_x emissions generally account for less than 5% of total anthropogenic emissions.[52] The soil NO_x emissions, up to 20% of anthropogenic sources but considered conventionally as biogenic sources (Figure S6), require additional attention in designing the emission control strategies.[57]

Sectoral influences on health burden vary among regions and seasons, with solvent VOC contributions to anthropogenically sourced O_3 health burden ranging from 3.9% in North Africa/Middle East to 19.2% in East Asia annually (Figure 2b) and reaching a peak of 33.5% in High Income Asia Pacific in the winter (Figure S7). These results highlight the importance of spatially and temporally dependent policies in emission control and health management. Taking East Asia as an example, targeted reduction of transportation NO_x emissions in winter ($PM_{2.5}$ as the main pollution species) and industry NO_x

https://doi.org/10.1021/acs.est.4c00339
Environ. Sci. Technol. 2024, 58, 11256−11267

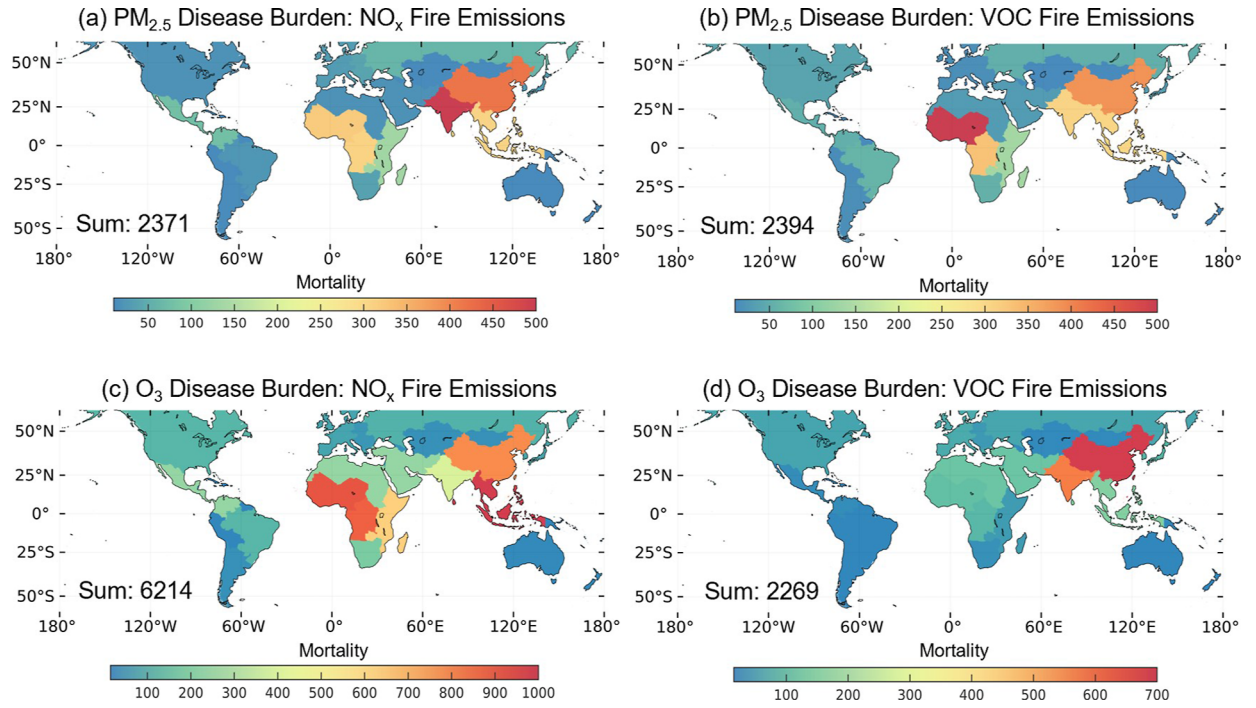

Figure 5. Impacts from NO_x and VOC fire emissions to mortalities attributed to $PM_{2.5}$ and O_3 exposure in the year 2019. Attributable global total numbers are given inset.

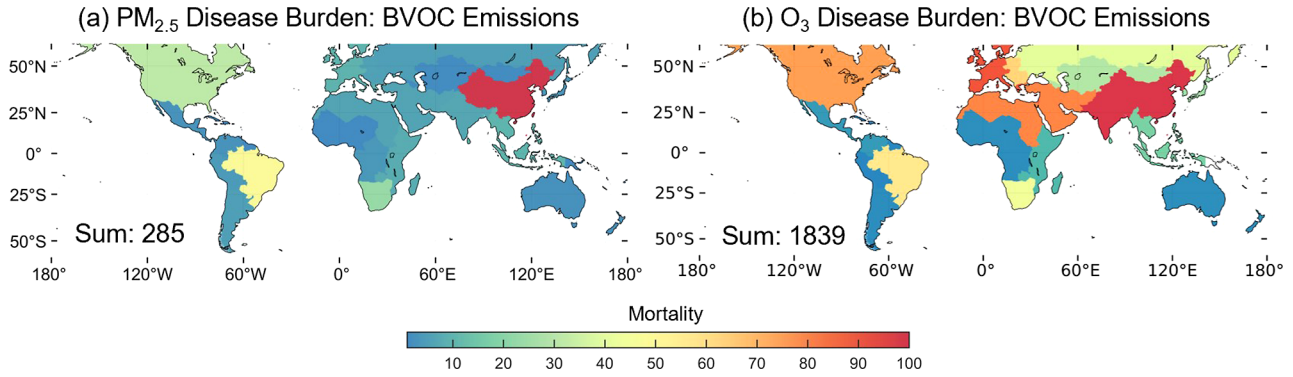

Figure 6. Impacts from biogenic VOC emissions to mortalities attributed to $PM_{2.5}$ and O_3 exposure during heatwave days in the year 2019. Attributable global total numbers are given in the inset.

emissions in summer (O_3 as the dominant species) may bring the highest health benefits, which can be complicated by the possible extension of the O_3 pollution season into winter,[58] when solvent VOC emissions play the dominant role (Figures 4 and S7).

3.3. Fire Sources. Fire-sourced emissions, mostly associated with agricultural biomass burning activities in middle−high latitudes in the northern hemisphere and with savanna, grassland, and shrubland fires in the tropical and southern hemisphere (Figure S8), are heavily tied to air pollution and health burden.[59] Fire episodes present soaring $PM_{2.5}$ (by up to 574.1 $\mu g\ m^{-3}$) and O_3 (by up to 334.7 $\mu g\ m^{-3}$) concentrations in 2019 (Figure S9). In turn, fire-sourced NO_x and VOC emissions, respectively, contribute to 8.5 (95% CI: 6.2−11.7) thousand and 4.8 (3.6−5.9) thousand mortalities worldwide, particularly for tropics with elevated vulnerability to climate change (Figure 5).

In Southeast Asia alone, 1.2 (95% CI: 0.9−1.6) thousand O_3-introduced mortalities could be avoided by eliminating fire NO_x emissions, with an additional 2.6 (1.9−4.4) thousand avoidable for Africa and 433 (261−645) avoidable for Latin America (Figure 5c). The broadly higher fire-sourced O_3 health burden relative to $PM_{2.5}$ is consistent with regional studies.[17] It should be noted that, in addition to NO_x and VOCs, fires also emit large amounts of primary pollutants, such as black carbon, organic carbon, and carbon monoxide, resulting in the potential for increased $PM_{2.5}$ and O_3 health burden.[60] Accordingly, collaboration under an international agreement to reduce fire-sourced emissions needs to be adopted to effectively control $PM_{2.5}$- and O_3-related health burden.

For South Asia and East Asia, with large mortality rates and high anthropogenic contributions (Figures 1 and 3), exposure to $PM_{2.5}$ and O_3 pollution caused by agricultural biomass burning brings a total of 3.7 (95% CI: 3.3−5.1) thousand mortalities. More importantly, unequal contributions from fire NO_x and VOC emissions address episode- and region-dependent strategies to control $PM_{2.5}$ and O_3 pollution and mitigate climate change in a coordinated way.

https://doi.org/10.1021/acs.est.4c00339
Environ. Sci. Technol. 2024, 58, 11256−11267

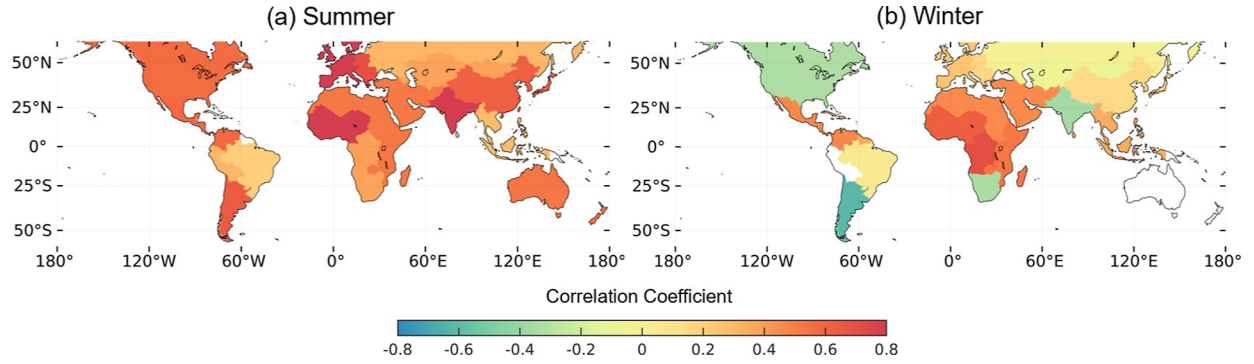

Figure 7. Correlation coefficients between daily $PM_{2.5}$ and O_3 health burdens in 2019. Results are shown for summer (June−August in the northern hemisphere and December−February in the southern hemisphere) and winter (December−February in the northern hemisphere and June−August in the southern hemisphere). Data samples of less than 10 are excluded from the analysis.

3.4. Heatwave-Related Biogenic Sources. The frequency, intensity, and duration of heatwaves are on the rise with the warming climate.[61] 2019 witnesses an average temperature 1.1 °C above the preindustrial period[62] and records widespread heatwave hotspots in middle−high latitudes (Figure S10). Here, a heatwave is defined as a daily maximum temperature exceeding the climatological average by 5 °C with a duration of 5 days or more.[63] Maximum temperatures lower than 30 °C are filtered out for the analysis. In response to the high temperature, intensive solar radiation, and stagnant anticyclonic conditions, increased biogenic VOC contributions to $PM_{2.5}$ and O_3 formation have drawn regional interest, emphasizing the dual role of vegetation for urban air quality.[64,65]

While $PM_{2.5}$-related mortalities (285 [95% CI: 235−341] globally) are mainly located in East Asia, the amplitude and coverage of biogenic VOC influences on health burden are notably larger for O_3 exposure (1839 [1498−2222]; Figure 6). For high-income regions with a generally heavier O_3 health burden in comparison to $PM_{2.5}$, such as High-Income North America and Western Europe (Figure 2), the O_3-related mortalities contributed by biogenic VOC episodically during heatwave events (75 [95% CI: 61−89] and 91 [79−103], respectively) are around 13% of those contributed by anthropogenic VOC annually (558 [364−749] and 722 [524−957]). In these cases, urban landscaping needs to be cautiously planned under changing climate. For other vulnerable and populated regions, the potential interaction between ambient high temperatures and air pollutants ($PM_{2.5}$ and O_3 concentrations by up to 19 and 3 times of WHO AQG levels; Figure S11) might generate a double-negative impact on public health.[66,67] Accordingly, a synergistic temperature-pollution warning system and event-targeted emission control actions, considering both biogenic sources and anthropogenic power emissions,[54] are required, particularly for sensitive individuals of the greatest health concern.

3.5. Implications for Future Emission Control and Health Management. Despite the increasing awareness of controlling anthropogenic NO_x and VOC emissions and long-term efforts to alleviate $PM_{2.5}$ and O_3 pollution,[19,68] health burden attributable to their short-term exposure remains high. Moreover, variations in daily $PM_{2.5}$ and O_3 health burden are positively correlated in most regions in summer with high levels of climate vulnerability (Figure 7), pinpointing the similar meteorological effects and shared precursor emissions, such as transportation, energy, and industry. Meanwhile, dual-pollutant joint control is needed for Asia, Europe, and North America in the winter season when $PM_{2.5}$ and O_3 show insignificant or negative correlations, resulting from reduced photolysis rates and the strong titration effect of O_3 pollution.[69]

Projected to 2050 in the International Energy Outlook,[70] the rapidly growing Africa and Middle East will be home to 2.8 billion residents (Figure 8a), comparable to the populations of India and China combined. Assuming invariable emission intensity and baseline mortalities relative to 2019, short-term exposure to $PM_{2.5}$ and O_3 is associated with a total health burden of 13.2 (95% CI: 7.2−16.8) mortalities per 100 thousand population. Targeted anthropogenic sources include NO_x emissions from transport (4.2% of total health burden), energy (2.7%), and industrial (1.4%) sectors (Figure 2), and natural NO_x and VOC sources likely play important roles during extreme events (Figures 5 and 6). In the future, increasing renewable energy from 5.7 quadrillion British thermal units (BTU) to 19.9 quadrillion BTU in Africa and the Middle East is technically and economically feasible (Figure 8d) to reduce $PM_{2.5}$ and O_3 health burden and improve climate change resilience under the consideration of distinct solution spaces and green growth pathways for each country.[71]

For East Asia and South Asia, with the present-day largest $PM_{2.5}$ and O_3 mortality rates, economic growth is expected to continue at a high pace (Figure 8b). Such projection drives future increases in energy generation and consumption for transportation and industry, respectively, by 1.5 and 1.3 times (Figure 8e−f), which currently account for 71.7% of the health burden attributable to anthropogenic NO_x and VOC influences. Despite the commonly increasing shares of renewable energy, the two major coal consumer countries, China and India, face a contrary evolution in future coal consumption (Figure S12), reflecting differences in energy efficiency, energy structure, and environmental regulations. Nevertheless, considering the current large amplitude of coal-based energy consumption (55.2% of global coal consumption; Figure S12) and the high fraction of energy-intensive manufacturing (66.7% of total industrial energy consumption; Figure S13) in China, cleaner power production is still an emergency.[4]

For high-income regions in North America and Western Europe, with shorter exposure durations and lower air pollution concentrations but considerable mortalities (Figure 2), effectively managing transportation NO_x and VOC emissions would substantially reduce the $PM_{2.5}$ and the O_3 health burden (9.3%). In the outlook, the reduction of on-road transportation energy consumption in the Americas and Europe will reverse around 2035 (Figure 8e), and the fraction of gasoline or E85

https://doi.org/10.1021/acs.est.4c00339
Environ. Sci. Technol. 2024, 58, 11256−11267

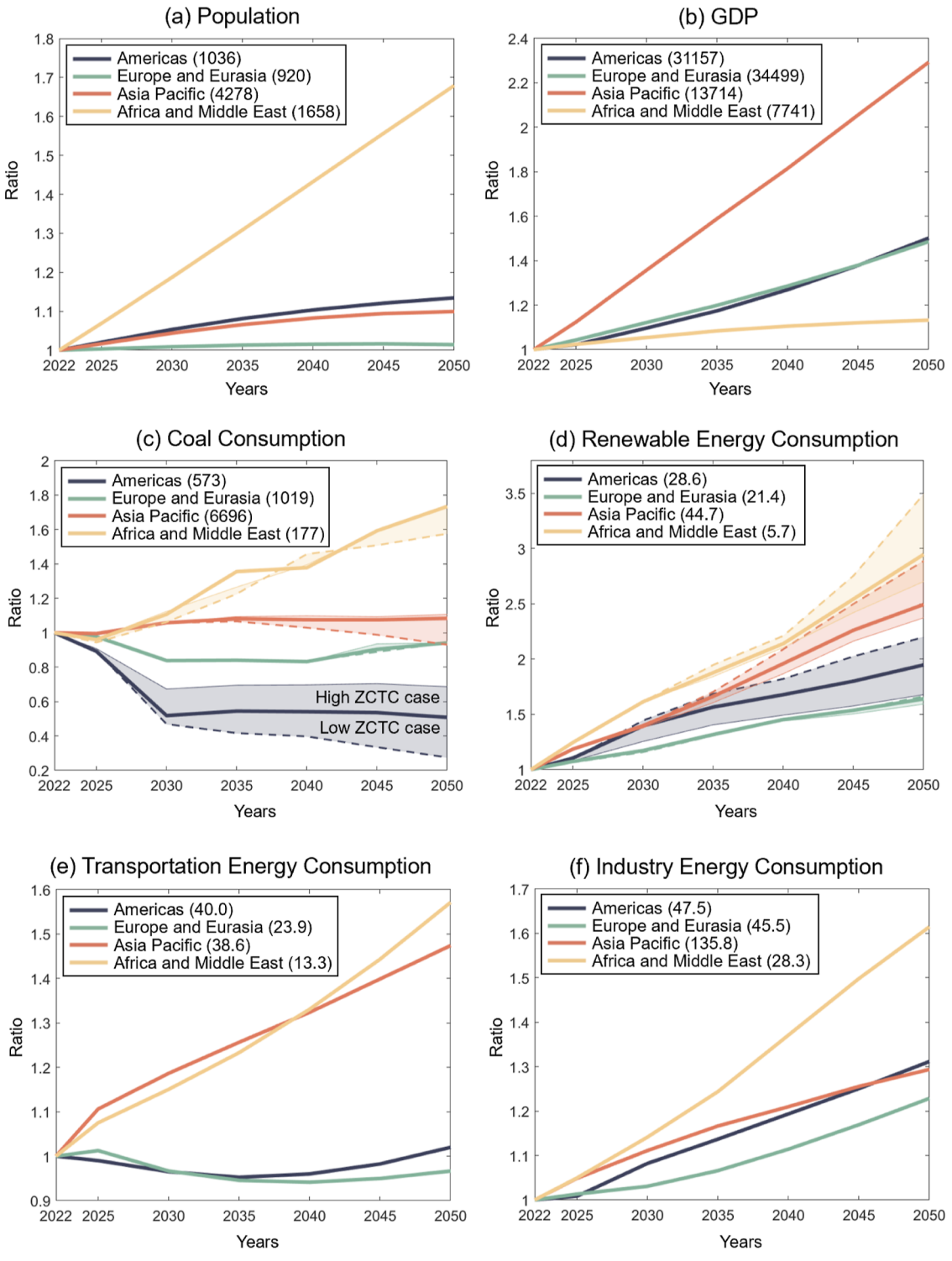

Figure 8. Future projections of social-economic indicators and energy-related parameters by region. Results are shown for population (a), gross domestic product per capita expressed in purchasing power parity (b), coal consumption (c), renewable energy consumption (d), transportation energy consumption (e), and industry energy consumption (f). Values are normalized with respect to 2022, and the absolute values of 2022 are given in parentheses. Units are million persons (a), 2015 dollars per person (PPP) (b), million short tons (c), and quadrillion British thermal units (BTU) (d–f). The data are taken from the U.S. Energy Information Administration (http://www.eia.gov/aeo). Solid lines show reference projections assuming current energy trends and relationships, existing laws and regulations, and economic and technological changes. Shadows in (b,c) show cases with high (solid edge) and low (dashed edge) zero-carbon technology cost.

fuels will remain relatively unreduced (48.8% in 2022 and 43.4% in 2050 of all fuels; Figure S14). Actions to increase the share of electric vehicles may offer options for rapid improvement in air quality and attributable health burden in high-income areas.[68]

In summary, reducing fuel-related emissions potentially provides immediate health benefits. With lessons learned from the Americas in Figure 8c–d and China and India in Figure S12, continuous economic development and technological innova-

https://doi.org/10.1021/acs.est.4c00339
Environ. Sci. Technol. 2024, 58, 11256−11267

tion, as well as investment for emission control, are key points for pollution control and health management. Taking Americas as an example, the low zero-carbon technology cost (ZCTC) case, assuming a more rapid capital cost decline, projects to more effectively replace coal (158.0 quadrillion BTU relative to 394.0 quadrillion BTU in the high ZCTC case) with renewable consumption (62.9 quadrillion BTU relative to 48.0 quadrillion BTU) to meet the energy demand and bring potential health benefits. It is noted that the projections are generated using the World Energy Projection System,[72] an integrated economic model representing policy-neutral baselines with assumptions of current policies and addressing the uncertainty by including cases with different macroeconomic growth, crude oil prices, as well as costs for zero-carbon generating technologies. Such projects are possibly shifted by new policy developments, technological breakthroughs, or geopolitical events.

3.6. Uncertainties. Our estimates of sectoral contributions and health burden represent their actual influences, including the pure contributions and interactional effects with other sources.[51] Uncertainties remain in the conclusions resulting from our use of the zeroing-out method since the total estimates can be biased as individual perturbation simulation may not capture the interactional effects among several different sources,[24] particularly for O_3 as a result of nonlinear compensating effects from emission sectors.[25] The combination with tagging possibly benefits the study by revealing how the contribution of sectoral sources to pollutant changes in response to mitigation measures. However, this should not downplay the significance of current findings in terms of policy implications. Second, despite our focus on region-scale strategies, the estimation of sectoral impacts is potentially limited by the spatial resolution of GEOS-Chem simulations, and further country- or city-level analysis can be improved with high-resolution nested simulations, particularly for extreme air pollution episodes (e.g., fires and heatwaves). Moreover, the assumption of the same toxicity of each source sector and relative risk across the globe can be improved under future developments of source- and country-specific, age- and gender-dependent epidemiologic studies on the global scale.[16,73]

■ ASSOCIATED CONTENT

Supporting Information

The Supporting Information is available free of charge at https://pubs.acs.org/doi/10.1021/acs.est.4c00339.

Data sources for exposure assessment; exposure performance evaluation; GEOS-Chem simulation evaluation; high-resolution mortality rate; seasonal sectoral impacts; agricultural and soil emissions; fire durations and types; pollution during fires; heatwave durations and temperatures; pollution during heatwaves; energy-related parameters by country or fuel; anthropogenic impacts on health burden by sector; and previous works (PDF)

■ AUTHOR INFORMATION

Corresponding Author

Lei Zhu − *School of Environmental Science and Engineering, Southern University of Science and Technology, Shenzhen 518055, China; Guangdong Provincial Observation and Research Station for Coastal Atmosphere and Climate of the Greater Bay Area, Shenzhen 518055, China; Shenzhen Key Laboratory of Precision Measurement and Early Warning Technology for Urban Environmental Health Risks, School of Environmental Science and Engineering, Southern University of Science and Technology, Shenzhen 518055, China;* Email: zhul3@sustech.edu.cn

Authors

Song Liu − *School of Environmental Science and Engineering, Southern University of Science and Technology, Shenzhen 518055, China; Collaborative Innovation Center of Atmospheric Environment and Equipment Technology, Jiangsu Key Laboratory of Atmospheric Environment Monitoring and Pollution Control (AEMPC), Nanjing University of Information Science and Technology, Nanjing 210044, China;* orcid.org/0000-0002-4063-0205

Xicheng Li − *School of Environmental Science and Engineering, Southern University of Science and Technology, Shenzhen 518055, China*

Jing Wei − *Department of Atmospheric and Oceanic Science, Earth System Science Interdisciplinary Center, University of Maryland, College Park, Maryland 20742-5031, United States*

Lei Shu − *School of Geographical Sciences, Fujian Normal University, Fuzhou 350117, China;* orcid.org/0000-0002-4099-8958

Jianbing Jin − *Jiangsu Key Laboratory of Atmospheric Environment Monitoring and Pollution Control, Collaborative Innovation Center of Atmospheric Environment and Equipment Technology, School of Environmental Science and Engineering, Nanjing University of Information Science and Technology, Nanjing 210044, China*

Tzung-May Fu − *School of Environmental Science and Engineering, Southern University of Science and Technology, Shenzhen 518055, China; Guangdong Provincial Observation and Research Station for Coastal Atmosphere and Climate of the Greater Bay Area, Shenzhen 518055, China; Shenzhen Key Laboratory of Precision Measurement and Early Warning Technology for Urban Environmental Health Risks, School of Environmental Science and Engineering, Southern University of Science and Technology, Shenzhen 518055, China;* orcid.org/0000-0002-8556-7326

Xin Yang − *School of Environmental Science and Engineering, Southern University of Science and Technology, Shenzhen 518055, China; Guangdong Provincial Observation and Research Station for Coastal Atmosphere and Climate of the Greater Bay Area, Shenzhen 518055, China; Shenzhen Key Laboratory of Precision Measurement and Early Warning Technology for Urban Environmental Health Risks, School of Environmental Science and Engineering, Southern University of Science and Technology, Shenzhen 518055, China;* orcid.org/0000-0002-9173-1188

Complete contact information is available at: https://pubs.acs.org/10.1021/acs.est.4c00339

Notes

The authors declare no competing financial interest.

■ ACKNOWLEDGMENTS

This work is funded by the National Natural Science Foundation of China (42205134 and 42375090), the Ministry of Science and Technology of the People's Republic of China (2023YFE0112900), the Guangdong Basic and Applied Basic Research Foundation (2024A1515011951), the Key-Area Research and Development Program of Guangdong Province (2020B1111360001), the Shenzhen Key Laboratory of

Precision Measurement and Early Warning Technology for Urban Environmental Health Risks (ZDSYS20220606100604008), the Guangdong Basic and Applied Basic Research Foundation (2021A1515110713), the Guangdong Basic and Applied Basic Research Fund (2020B1515130003), the Guangdong University Research Project Science Team (2021KCXTD004), the Shenzhen Science and Technology Program (KQTD20210811090048025, JCYJ20210324104604012, and JCYJ20220530115404009), the High level of special funds (G030290001), and the Jiangsu Key Laboratory of Atmospheric Environment Monitoring and Pollution Control (KHK001). This work is supported by the Center for Computational Science and Engineering at Southern University of Science and Technology.

REFERENCES

(1) GBD. 2019 Risk Factors Collaborators Global burden of 87 risk factors in 204 countries and territories, 1990−2019: a systematic analysis for the Global Burden of Disease Study 2019. *Lancet* **2020**, *396*, 1223−1249.

(2) Atkinson, R. Atmospheric chemistry of VOCs and NO_x. *Atmos. Environ.* **2000**, *34*, 2063−2101.

(3) Butler, T.; Lupascu, A.; Nalam, A. Attribution of ground-level ozone to anthropogenic and natural sources of nitrogen oxides and reactive carbon in a global chemical transport model. *Atmos. Chem. Phys.* **2020**, *20*, 10707−10731.

(4) McDuffie, E. E.; Martin, R. V.; Spadaro, J. V.; Burnett, R.; Smith, S. J.; O'Rourke, P.; Hammer, M. S.; van Donkelaar, A.; Bindle, L.; Shah, V.; Jaeglé, L.; Luo, G.; Yu, F.; Adeniran, J. A.; Lin, J.; Brauer, M. Source sector and fuel contributions to ambient $PM_{2.5}$ and attributable mortality across multiple spatial scales. *Nat. Commun.* **2021**, *12*, 3594.

(5) Wei, J.; Li, Z.; Chen, X.; Li, C.; Sun, Y.; Wang, J.; Lyapustin, A.; Brasseur, G.; Jiang, M.; Sun, L.; Wang, T.; Jung, C.; Qiu, B.; Fang; Liu, X.; Hao, J.; Wang, Y.; Zhan, M.; Song, X.; Liu, Y. Separating daily 1 km $PM_{2.5}$ inorganic chemical composition in China since 2000 via deep learning integrating ground, satellite, and model data. *Environ. Sci. Technol.* **2023**, *57* (46), 18282−18295.

(6) Geng, G.; Xiao, Q.; Liu, S.; Liu, X.; Cheng, J.; Zheng, Y.; Xue, T.; Tong, D.; Zheng, B.; Peng, Y.; Huang, X.; He, K.; Zhang, Q. Tracking air pollution in China: near real-time $PM_{2.5}$ retrievals from multisource data fusion. *Environ. Sci. Technol.* **2021**, *55*, 12106−12115.

(7) Lu, X.; Hong, J.; Zhang, L.; Cooper, O. R.; Schultz, M. G.; Xu, X.; Wang, T.; Gao, M.; Zhao, Y.; Zhang, Y. Severe surface ozone pollution in China: a global perspective. *Environ. Sci. Technol. Lett.* **2018**, *5*, 487−494.

(8) Zhu, S.; Xu, J.; Zeng, J.; Yu, C.; Wang, Y.; Yan, H. Satellite-derived estimates of surface ozone by LESO: Extended application and performance evaluation. *Int. J. Appl. Earth Obs. Geoinf.* **2022**, *113*, 103008.

(9) Xiao, Q.; Geng, G.; Xue, T.; Liu, S.; Cai, C.; He, K.; Zhang, Q. Tracking $PM_{2.5}$ and O_3 pollution and the related health burden in China 2013−2020. *Environ. Sci. Technol.* **2022**, *56*, 6922−6932.

(10) Wang, F.; Qiu, X.; Cao, J.; Peng, L.; Zhang, N.; Yan, Y.; Li, R. Policy-driven changes in the health risk of $PM_{2.5}$ and O_3 exposure in China during 2013−2018. *Sci. Total Environ.* **2021**, *757*, 143775.

(11) Lu, X.; Zhang, L.; Yue, X.; Zhang, J.; Jaffe, D. A.; Stohl, A.; Zhao, Y.; Shao, J. Wildfire influences on the variability and trend of summer surface ozone in the mountainous western United States. *Atmos. Chem. Phys.* **2016**, *16*, 14687−14702.

(12) Ma, M.; Gao, Y.; Wang, Y.; Zhang, S.; Leung, L. R.; Liu, C.; Wang, S.; Zhao, B.; Chang, X.; Su, H.; Zhang, T.; Sheng, L.; Yao, X.; Gao, H. Substantial ozone enhancement over the North China Plain from increased biogenic emissions due to heat waves and land cover in summer 2017. *Atmos. Chem. Phys.* **2019**, *19*, 12195−12207.

(13) Ryan, R. G.; Marais, E. A.; Gershenson-Smith, E.; Ramsay, R.; Muller, J.-P.; Tirpitz, J.-L.; Frieß, U. Measurement Report: MAX-DOAS measurements characterise Central London ozone pollution episodes during 2022 heatwaves. *Atmos. Chem. Phys.* **2023**, *23*, 7121−7139.

(14) Stedman, J. R. The predicted number of air pollution related deaths in the UK during the August 2003 heatwave. *Atmos. Environ.* **2004**, *38*, 1087−1090.

(15) Fann, N.; Alman, B.; Broome, R. A.; Morgan, G. G.; Johnston, F. H.; Pouliot, G.; Rappold, A. G. The health impacts and economic value of wildland fire episodes in the US: 2008−2012. *Sci. Total Environ.* **2018**, *610*−*611*, 802−809.

(16) Chen, G.; Guo, Y.; Yue, X.; Tong, S.; Gasparrini, A.; Bell, M. L.; Armstrong, B.; Schwartz, J.; Jaakkola, J. J.; Zanobetti, A.; et al. others Mortality risk attributable to wildfire-related $PM_{2.5}$ pollution: a global time series study in 749 locations. *Lancet Planet. Health* **2021**, *5*, e579−e587.

(17) Zhou, B.; Knote, C. An estimate of excess mortality resulting from air pollution caused by wildfires in the eastern and central Mediterranean basin in 2021. *Nat. Hazards Earth Syst. Sci. Discuss.* **2023**, 1−44.

(18) Wang, Y.; Wild, O.; Chen, X.; Wu, Q.; Gao, M.; Chen, H.; Qi, Y.; Wang, Z. Health impacts of long-term ozone exposure in China over 2013−2017. *Environ. Int.* **2020**, *144*, 106030.

(19) Li, C.; van Donkelaar, A.; Hammer, M. S.; McDuffie, E. E.; Burnett, R. T.; Spadaro, J. V.; Chatterjee, D.; Cohen, A. J.; Apte, J. S.; Southerland, V. A.; Anenberg, S. C.; Brauer, M.; Martin, R. V. Reversal of trends in global fine particulate matter air pollution. *Nat. Commun.* **2023**, *14*, 5349.

(20) Wei, J.; Li, Z.; Li, K.; Dickerson, R. R.; Pinker, R. T.; Wang, J.; Liu, X.; Sun, L.; Xue, W.; Cribb, M. Full-coverage mapping and spatiotemporal variations of ground-level ozone (O_3) pollution from 2013 to 2020 across China. *Rem. Sens. Environ.* **2022**, *270*, 112775.

(21) Wei, J.; Li, Z.; Lyapustin, A.; Wang, J.; Dubovik, O.; Schwartz, J.; Sun, L.; Li, C.; Liu, S.; Zhu, T. First close insight into global daily gapless 1 km $PM_{2.5}$ pollution, driving factors, and health impact. *Nat. Commun.* **2023**, *14*, 8349.

(22) Gao, M.; Gao, J.; Zhu, B.; Kumar, R.; Lu, X.; Song, S.; Zhang, Y.; Jia, B.; Wang, P.; Beig, G.; Hu, J.; Ying, Q.; Zhang, H.; Sherman, P.; McElroy, M. B. Ozone pollution over China and India: seasonality and sources. *Atmos. Chem. Phys.* **2020**, *20*, 4399−4414.

(23) Li, P.; Yang, Y.; Wang, H.; Li, S.; Li, K.; Wang, P.; Li, B.; Liao, H. Source attribution of near-surface ozone trends in the United States during 1995−2019. *Atmos. Chem. Phys.* **2023**, *23*, 5403−5417.

(24) Lu, X.; Zhang, L.; Chen, Y.; Zhou, M.; Zheng, B.; Li, K.; Liu, Y.; Lin, J.; Fu, T.-M.; Zhang, Q. Exploring 2016−2017 surface ozone pollution over China: source contributions and meteorological influences. *Atmos. Chem. Phys.* **2019**, *19*, 8339−8361.

(25) Grewe, V.; Dahlmann, K.; Matthes, S.; Steinbrecht, W. Attributing ozone to NO_x emissions: Implications for climate mitigation measures. *Atmos. Environ.* **2012**, *59*, 102−107.

(26) Geurts, P.; Ernst, D.; Wehenkel, L. Extremely randomized trees. *Mach. Learn.* **2006**, *63*, 3−42.

(27) Lelieveld, J.; Barlas, C.; Giannadaki, D.; Pozzer, A. Model calculated global, regional and megacity premature mortality due to air pollution. *Atmos. Chem. Phys.* **2013**, *13*, 7023−7037.

(28) Dedoussi, I. C.; Eastham, S. D.; Monier, E.; Barrett, S. R. Premature mortality related to United States cross-state air pollution. *Nature* **2020**, *578*, 261−265.

(29) Anenberg, S. C.; Horowitz, L. W.; Tong, D. Q.; West, J. J. An estimate of the global burden of anthropogenic ozone and fine particulate matter on premature human mortality using atmospheric modeling. *Environ. Health Perspect.* **2010**, *118*, 1189−1195.

(30) Orellano, P.; Reynoso, J.; Quaranta, N.; Bardach, A.; Ciapponi, A. Short-term exposure to particulate matter (PM_{10} and $PM_{2.5}$), nitrogen dioxide (NO_2), and ozone (O_3) and all-cause and cause-specific mortality: Systematic review and meta-analysis. *Environ. Int.* **2020**, *142*, 105876.

(31) Gelaro, R.; McCarty, W.; Suárez, M. J.; Todling, R.; Molod, A.; Takacs, L.; Randles, C. A.; Darmenov, A.; Bosilovich, M. G.; Reichle, R.; Wargan, K.; Coy, L.; Cullather, R.; Draper, C.; Akella, S.; Buchard,

https://doi.org/10.1021/acs.est.4c00339
Environ. Sci. Technol. 2024, 58, 11256−11267

V.; Conaty, A.; da Silva, A. M.; Gu, W.; Kim, G.-K.; Koster, R.; Lucchesi, R.; Merkova, D.; Nielsen, J. E.; Partyka, G.; Pawson, S.; Putman, W.; Rienecker, M.; Schubert, S. D.; Sienkiewicz, M.; Zhao, B. The modern-era retrospective analysis for research and applications, version 2 (MERRA-2). *J. Clim.* **2017**, *30*, 5419−5454.

(32) Hoesly, R. M.; Smith, S. J.; Feng, L.; Klimont, Z.; Janssens-Maenhout, G.; Pitkanen, T.; Seibert, J. J.; Vu, L.; Andres, R. J.; Bolt, R. M.; Bond, T. C.; Dawidowski, L.; Kholod, N.; Kurokawa, J.-I.; Li, M.; Liu, L.; Lu, Z.; Moura, M. C. P.; O'Rourke, P. R.; Zhang, Q. Historical (1750−2014) anthropogenic emissions of reactive gases and aerosols from the Community Emissions Data System (CEDS). *Geosci. Model Dev.* **2018**, *11*, 369−408.

(33) Hudman, R.; Moore, N.; Mebust, A.; Martin, R.; Russell, A.; Valin, L.; Cohen, R. Steps towards a mechanistic model of global soil nitric oxide emissions: implementation and space based-constraints. *Atmos. Chem. Phys.* **2012**, *12*, 7779−7795.

(34) Guenther, A.; Jiang, X.; Heald, C. L.; Sakulyanontvittaya, T.; Duhl, T.; Emmons, L.; Wang, X. The Model of Emissions of Gases and Aerosols from Nature version 2.1 (MEGAN2.1): an extended and updated framework for modeling biogenic emissions. *Geosci. Model Dev.* **2012**, *5*, 1471−1492.

(35) Giglio, L.; Randerson, J. T.; Van Der Werf, G. R. Analysis of daily, monthly, and annual burned area using the fourth-generation global fire emissions database (GFED4). *J. Geophys. Res.: Biogeosci.* **2013**, *118*, 317−328.

(36) Bey, I.; Jacob, D. J.; Yantosca, R. M.; Logan, J. A.; Field, B. D.; Fiore, A. M.; Li, Q.; Liu, H. Y.; Mickley, L. J.; Schultz, M. G. Global modeling of tropospheric chemistry with assimilated meteorology: Model description and evaluation. *J. Geophys. Res. Atmos.* **2001**, *106*, 23073−23095.

(37) Park, R. J.; Jacob, D. J.; Field, B. D.; Yantosca, R. M.; Chin, M. Natural and transboundary pollution influences on sulfate-nitrate-ammonium aerosols in the United States: Implications for policy. *J. Geophys. Res. Atmos.* **2004**, *109*..

(38) Mao, J.; Paulot, F.; Jacob, D. J.; Cohen, R. C.; Crounse, J. D.; Wennberg, P. O.; Keller, C. A.; Hudman, R. C.; Barkley, M. P.; Horowitz, L. W. Ozone and organic nitrates over the eastern United States: Sensitivity to isoprene chemistry. *J. Geophys. Res. Atmos.* **2013**, *118*, 11−256.

(39) Sherwen, T.; Schmidt, J. A.; Evans, M. J.; Carpenter, L. J.; Großmann, K.; Eastham, S. D.; Jacob, D. J.; Dix, B.; Koenig, T. K.; Sinreich, R.; Ortega, I.; Volkamer, R.; Saiz-Lopez, A.; Prados-Roman, C.; Mahajan, A. S.; Ordóñez, C. Global impacts of tropospheric halogens (Cl, Br, I) on oxidants and composition in GEOS-Chem. *Atmos. Chem. Phys.* **2016**, *16*, 12239−12271.

(40) Martin, R. V.; Jacob, D. J.; Yantosca, R. M.; Chin, M.; Ginoux, P. Global and regional decreases in tropospheric oxidants from photochemical effects of aerosols. *J. Geophys. Res. Atmos.* **2003**, *108*, 4097.

(41) Fountoukis, C.; Nenes, A. ISORROPIA II: a computationally efficient thermodynamic equilibrium model for K^+<−Ca^{2+}<−Mg^{2+}<−NH_4^+<−Na^+<−SO_4^{2-}<−NO_3^-<−<−Cl^-<−<−H_2O aerosols. *Atmos. Chem. Phys.* **2007**, *7*, 4639−4659.

(42) Pye, H.; Liao, H.; Wu, S.; Mickley, L. J.; Jacob, D. J.; Henze, D. K.; Seinfeld, J. Effect of changes in climate and emissions on future sulfate-nitrate-ammonium aerosol levels in the United States. *J. Geophys. Res. Atmos.* **2009**, *114*, D01205.

(43) Pai, S. J.; Heald, C. L.; Pierce, J. R.; Farina, S. C.; Marais, E. A.; Jimenez, J. L.; Campuzano-Jost, P.; Nault, B. A.; Middlebrook, A. M.; Coe, H.; Shilling, J. E.; Bahreini, R.; Dingle, J. H.; Vu, K. An evaluation of global organic aerosol schemes using airborne observations. *Atmos. Chem. Phys.* **2020**, *20*, 2637−2665.

(44) Park, R. J.; Jacob, D. J.; Chin, M.; Martin, R. V. Sources of carbonaceous aerosols over the United States and implications for natural visibility. *J. Geophys. Res. Atmos.* **2003**, *108*, 4355.

(45) Fairlie, T. D.; Jacob, D. J.; Park, R. J. The impact of transpacific transport of mineral dust in the United States. *Atmos. Environ.* **2007**, *41*, 1251−1266.

(46) Jaeglé, L.; Quinn, P.; Bates, T.; Alexander, B.; Lin, J.-T. Global distribution of sea salt aerosols: new constraints from in situ and remote sensing observations. *Atmos. Chem. Phys.* **2011**, *11*, 3137−3157.

(47) Boersma, K.; Jacob, D. J.; Trainic, M.; Rudich, Y.; DeSmedt, I.; Dirksen, R.; Eskes, H. Validation of urban NO_2 concentrations and their diurnal and seasonal variations observed from the SCIAMACHY and OMI sensors using in situ surface measurements in Israeli cities. *Atmos. Chem. Phys.* **2009**, *9*, 3867−3879.

(48) Zhu, L.; Jacob, D. J.; Kim, P. S.; Fisher, J. A.; Yu, K.; Travis, K. R.; Mickley, L. J.; Yantosca, R. M.; Sulprizio, M. P.; De Smedt, I.; González Abad, G.; Chance, K.; Li, C.; Ferrare, R.; Fried, A.; Hair, J. W.; Hanisco, T. F.; Richter, D.; Jo Scarino, A.; Walega, J.; Weibring, P.; Wolfe, G. M. Observing atmospheric formaldehyde (HCHO) from space: validation and intercomparison of six retrievals from four satellites (OMI, GOME2A, GOME2B, OMPS) with SEAC^{4}RS aircraft observations over the southeast US. *Atmos. Chem. Phys.* **2016**, *16*, 13477−13490.

(49) David, L. M.; Ravishankara, A.; Brewer, J. F.; Sauvage, B.; Thouret, V.; Venkataramani, S.; Sinha, V. Tropospheric ozone over the Indian subcontinent from 2000 to 2015: Data set and simulation using GEOS-Chem chemical transport model. *Atmos. Environ.* **2019**, *219*, 117039.

(50) Fritz, T. M.; Eastham, S. D.; Emmons, L. K.; Lin, H.; Lundgren, E. W.; Goldhaber, S.; Barrett, S. R. H.; Jacob, D. J. Implementation and evaluation of the GEOS-Chem chemistry module version 13.1.2 within the Community Earth System Model v2.1. *Geosci. Model Dev.* **2022**, *15*, 8669−8704.

(51) Li, N.; He, Q.; Greenberg, J.; Guenther, A.; Li, J.; Cao, J.; Wang, J.; Liao, H.; Wang, Q.; Zhang, Q. Impacts of biogenic and anthropogenic emissions on summertime ozone formation in the Guanzhong Basin, China. *Atmos. Chem. Phys.* **2018**, *18*, 7489−7507.

(52) McDuffie, E. E.; Smith, S. J.; O'Rourke, P.; Tibrewal, K.; Venkataraman, C.; Marais, E. A.; Zheng, B.; Crippa, M.; Brauer, M.; Martin, R. V. A global anthropogenic emission inventory of atmospheric pollutants from sector-and fuel-specific sources (1970−2017): an application of the Community Emissions Data System (CEDS). *Earth Syst. Sci. Data* **2020**, *12*, 3413−3442.

(53) Liu, S.; Li, X.; Li, J.; Shu, L.; Fu, T.-M.; Yang, X.; Zhu, L. Observing network effect of shipping emissions from space: A natural experiment in the world's busiest port. *PNAS Nexus* **2023**, *2*, pgad391.

(54) Liu, S.; Shu, L.; Zhu, L.; Song, Y.; Sun, W.; Chen, Y.; Wang, D.; Pu, D.; Li, X.; Sun, S.; Li, J.; Zuo, X.; Fu, W.; Yang, X.; Fu, T.-M. Underappreciated emission spikes from power plants during heatwaves observed from space: Case studies in India and China. *Earth's Future* **2024**, *12*, No. e2023EF003937.

(55) World Health Organization. *WHO Global Air Quality Guidelines: Particulate Matter ($PM_{2.5}$ and PM10), Ozone, Nitrogen Dioxide, Sulfur Ddioxide and Carbon Monoxide*; World Health Organization, 2021.

(56) Malashock, D. A.; DeLang, M. N.; Becker, J. S.; Serre, M. L.; West, J. J.; Chang, K.-L.; Cooper, O. R.; Anenberg, S. C. Estimates of ozone concentrations and attributable mortality in urban, peri-urban and rural areas worldwide in 2019. *Environ. Res. Lett.* **2022**, *17*, 054023.

(57) Lu, X.; Ye, X.; Zhou, M.; Zhao, Y.; Weng, H.; Kong, H.; Li, K.; Gao, M.; Zheng, B.; Lin, J.; Zhou, F.; Zhang, Q.; Wu, D.; Zhang, L.; Zhang, Y. The underappreciated role of agricultural soil nitrogen oxide emissions in ozone pollution regulation in North China. *Nat. Commun.* **2021**, *12*, 5021.

(58) Li, K.; Jacob, D. J.; Liao, H.; Qiu, Y.; Shen, L.; Zhai, S.; Bates, K. H.; Sulprizio, M. P.; Song, S.; Lu, X.; Zhang, Q.; Zheng, B.; Zhang, Y.; Zhang, J.; Lee, H. C.; Kuk, S. K. Ozone pollution in the North China Plain spreading into the late-winter haze season. *Proc. Natl. Acad. Sci. U.S.A.* **2021**, *118*, No. e2015797118.

(59) Xu, R.; Ye, T.; Yue, X.; Yang, Z.; Yu, W.; Zhang, Y.; Bell, M. L.; Morawska, L.; Yu, P.; Zhang, Y.; Wu, Y.; Liu, Y.; Johnston, F.; Lei, Y.; Abramson, M. J.; Guo, Y.; Li, S.; Li, S. Global population exposure to landscape fire air pollution from 2000 to 2019. *Nature* **2023**, *621*, 521−529.

(60) Wei, J.; Wang, J.; Li, Z.; Kondragunta, S.; Anenberg, S.; Wang, Y.; Zhang, H.; Diner, D.; Hand, J.; Lyapustin, A.; Kahn, R.; Colarco, P.; da Silva, A.; Ichoku, C. Long-term mortality burden trends attributed to

black carbon and $PM_{2.5}$ from wildfire emissions across the continental USA from 2000 to 2020: a deep learning modelling study. *Lancet Planet. Health* **2023**, *7*, e963−e975.
(61) Perkins-Kirkpatrick, S.; Lewis, S. Increasing trends in regional heatwaves. *Nat. Commun.* **2020**, *11*, 3357.
(62) *World Meteorological Organization WMO Statement on the State of the Gglobal Cclimate in 2019. WMO-No. 1248*; WHO, 2020.
(63) Frich, P.; Alexander, L. V.; Della-Marta, P.; Gleason, B.; Haylock, M.; Klein Tank, A.; Peterson, T. Observed coherent changes in climatic extremes during the second half of the twentieth century. *Clim. Res.* **2002**, *19*, 193−212.
(64) Churkina, G.; Kuik, F.; Bonn, B.; Lauer, A.; Grote, R.; Tomiak, K.; Butler, T. M. Effect of VOC emissions from vegetation on air quality in Berlin during a heatwave. *Environ. Sci. Technol.* **2017**, *51*, 6120−6130.
(65) Wang, H.; Wu, K.; Liu, Y.; Sheng, B.; Lu, X.; He, Y.; Xie, J.; Wang, H.; Fan, S. Role of heat wave-induced biogenic VOC enhancements in persistent ozone episodes formation in Pearl River Delta. *J. Geophys. Res. Atmos.* **2021**, *126*, No. e2020JD034317.
(66) Zong, L.; Yang, Y.; Xia, H.; Gao, M.; Sun, Z.; Zheng, Z.; Li, X.; Ning, G.; Li, Y.; Lolli, S. Joint occurrence of heatwaves and ozone pollution and increased health risks in Beijing, China: role of synoptic weather pattern and urbanization. *Atmos. Chem. Phys.* **2022**, *22*, 6523−6538.
(67) Zhou, L.; Wang, Y.; Wang, Q.; Ding, Z.; Jin, H.; Zhang, T.; Zhu, B. The interactive effects of extreme temperatures and $PM_{2.5}$ pollution on mortalities in Jiangsu Province, China. *Sci. Rep.* **2023**, *13*, 9479.
(68) Lyu, X.; Li, K.; Guo, H.; Morawska, L.; Zhou, B.; Zeren, Y.; Jiang, F.; Chen, C.; Goldstein, A. H.; Xu, X.; Wang, T.; Lu, X.; Zhu, T.; Querol, X.; Chatani, S.; Latif, M. T.; Schuch, D.; Sinha, V.; Kumar, P.; Mullins, B.; Seguel, R.; Shao, M.; Xue, L.; Wang, N.; Chen, J.; Gao, J.; Chai, F.; Simpson, I.; Sinha, B.; Blake, D. R. A synergistic ozone-climate control to address emerging ozone pollution challenges. *One Earth* **2023**, *6*, 964−977.
(69) Zhu, J.; Chen, L.; Liao, H.; Dang, R. Correlations between $PM_{2.5}$ and ozone over China and associated underlying reasons. *Atmosphere* **2019**, *10*, 352.
(70) U.S. Energy Information Administration, International Energy Outlook 2023, 2023. https://www.eia.gov/outlooks/ieo/pdf/IEO2023_Narrative.pdf.
(71) Mulugetta, Y.; Sokona, Y.; Trotter, P. A.; Fankhauser, S.; Omukuti, J.; Somavilla Croxatto, L.; Steffen, B.; Tesfamichael, M.; Abraham, E.; Adam, J.-P.; Agbemabiese, L.; Agutu, C.; Aklilu, M. P.; Alao, O.; Batidzirai, B.; Bekele, G.; Dagnachew, A. G.; Davidson, O.; Denton, F.; Diemuodeke, E. O.; Egli, F.; Eshetu, G. G.; Gebreslassie, M.; Goundiam, M.; Gujba, H. K.; Hailu, Y.; Hawkes, A. D.; Hirmer, S.; Hoka, H.; Howells, M.; Isah, A.; Kammen, D.; Kemausuor, F.; Khennas, I.; Kruger, W.; Malo, I.; Mofor, L.; Nago, M.; Nock, D.; Okereke, C.; Ouedraogo, S. N.; Probst, B.; Schmidt, M.; Schmidt, T. S.; Shenga, C.; Sokona, M.; Steckel, J. C.; Sterl, S.; Tembo, B.; Tomei, J.; Twesigye, P.; Watson, J.; Winkler, H.; Yussuff, A. Africa needs context-relevant evidence to shape its clean energy future. *Nat. Energy* **2022**, *7*, 1015−1022.
(72) U.S. Energy Information Administration. World Energy Projection System (WEPS): Overview, 2021. https://www.eia.gov/analysis/handbook/pdf/weps2021_overview.pdf.
(73) Alari, A.; Chen, C.; Schwarz, L.; Hdansen, K.; Chaix, B.; Benmarhnia, T. The Role of Ozone as a Mediator of the Relationship Between Heat Waves and Mortality in 15 French Urban Areas. *American Journal of Epidemiology* **2023**, *192*, 949−962.

https://doi.org/10.1021/acs.est.4c00339
Environ. Sci. Technol. 2024, 58, 11256−11267